26p

NASA

TECHNICAL NOTE

D-1804

PERFORMANCE OF A PLUG NOZZLE HAVING A

CONCAVE CENTRAL BASE WITH AND WITHOUT TERMINAL FAIRINGS

AT TRANSONIC SPEEDS

By Charles E. Mercer and Leland B. Salters, Jr.

Langley Research Center
Langley Station, Hampton, Va.

NATIONAL AERONAUTICS AND SPACE ADMINISTRATION

TECHNICAL NOTE D-1804

PERFORMANCE OF A PLUG NOZZLE HAVING A

CONCAVE CENTRAL BASE WITH AND WITHOUT TERMINAL FAIRINGS

AT TRANSONIC SPEEDS

By Charles E. Mercer and Leland B. Salters, Jr.

SUMMARY

    The performance of a plug nozzle with concave central base, with and without
terminal fairings, has been evaluated at transonic speeds. The basic nozzle had
a turning-lip angle of about 29°, a ratio of annular gap to base radius of 0.35,
and a ratio of annular gap to base depth of 13.8. The model was tested at zero
angle of attack at Mach numbers from 0.80 to 1.28 and at jet total-pressure ratios
from 1.00 to 8.20. A hot-jet exhaust was used.

    The overall efficiency of the configuration without terminal fairings
decreased with increase in Mach number in the pressure-ratio range of this
investigation. The terminal fairings decreased the thrust minus drag at subsonic
speeds but increased that for sonic and above-sonic speeds. The base flow pattern
influenced the concave-base thrust but not the overall thrust minus drag.

INTRODUCTION

    An investigation of the static propulsion characteristics of an annular noz-
zle with a concave central base has been conducted at the jet-exit test stand of
the Langley 16-foot transonic tunnel and the results are reported in references 1
and 2. The principle of operation of the annular nozzle with concave central base
is described in reference 1. The results of the static investigation were consid-
ered sufficiently promising to warrant an extension of the research to investigate
the effects of an external airstream. The present work is, therefore, a contin-
uation of the original investigation in that it consists of a study of the annu-
lar nozzle with concave central base at forward flight velocities. Also included
is an evaluation of the effects of terminal fairings (ref. 3) on the performance
of the basic nozzle. This work is related to the investigation of the isentropic-
plug-type nozzles reported in reference 4 in that the geometric shapes of the noz-
zle outer lip and the terminal fairings are identical.

    In this investigation, the basic model, with and without terminal fairings,
was tested at zero angle of attack at Mach numbers from 0.80 to 1.28 and at jet

total-pressure ratios from 1.00 to 8.20. The hot-jet exhaust was provided by a hydrogen peroxide turbojet-engine simulator of the type described in reference 5.

SYMBOLS

A_l local area, sq ft

A_{max} maximum cross-sectional area of body, sq ft

$C_{F,b}$ concave-base thrust coefficient, $\dfrac{F_b}{q_\infty A_{max}}$ for $M > 0$ or $\dfrac{F_b}{p_\infty A_{max}}$ for static conditions

$C_{F,i}$ ideal isentropic thrust coefficient, $\dfrac{F_i}{q_\infty A_{max}}$ for $M > 0$ or $\dfrac{F_i}{p_\infty A_{max}}$ for static conditions

$C_{(F-D)}$ measured thrust-minus-drag coefficient, $\dfrac{F - D}{q_\infty A_{max}}$ for $M > 0$ or $\dfrac{F - D}{p_\infty A_{max}}$ for static conditions

C_p concave-base pressure coefficient, $\dfrac{p_l - p_\infty}{q_\infty}$ for $M > 0$ or $\dfrac{p_l - p_\infty}{p_\infty}$ for static conditions

D drag, lb

F thrust, lb

F_b concave-base thrust, $\displaystyle\sum \left(p_l - p_\infty\right)A_l$, lb

F_i ideal thrust for complete isentropic expansion of jet flow,

$$w\sqrt{\frac{2R}{g}\frac{\gamma}{\gamma - 1}T_{t,j}\left[1 - \left(\frac{p_\infty}{p_{t,j}}\right)^{\frac{\gamma-1}{\gamma}}\right]}\text{, lb}$$

g gravitational acceleration, ft/sec^2; annulus-gap width, in.

l overhang of nozzle outer lip (0.04 in.)

M_∞ free-stream Mach number

p_l local static pressure, lb/sq ft

$p_{t,j}$ jet total pressure, lb/sq ft

p_∞ free-stream static pressure, lb/sq ft

q_∞ free-stream dynamic pressure, lb/sq ft

R gas constant (69.89 ft/$^\circ$R for 90-percent hydrogen peroxide products at $1,364^\circ$ F); concave-base radius, in.

R_1 radius to plug nozzle surface, in.

R_2 radius to inner surface of terminal fairings, in.

r radial distance from axis of symmetry to pressure orifice, in.

$T_{t,j}$ jet total temperature, $^\circ$R

w measured weight flow, lb/sec

x axial distance from jet exit, positive upstream, in.

z section width of terminal fairing, in.

γ ratio of specific heats (1.266 for 90-percent hydrogen peroxide products at $1,364^\circ$ F)

ϕ meridian angle, positive clockwise when viewed from point downstream of nozzle exit, deg

APPARATUS AND METHODS

This investigation was conducted in the Langley 16-foot transonic tunnel, which is a single-return atmospheric wind tunnel with an octagonal slotted test section and continuous air exchange. Two afterbody-nozzle configurations were tested and are depicted in figure 1. In each case an annular, plug-type nozzle was used with the downstream end of the plug contoured to form a concave base. The internal contours of the nozzles were identical. Configuration I had a relatively low boattail angle (10.5°) which resulted in a blunt physical base. This blunt base was removed on configuration II by increasing the boattail angle to 29.7°. This angle was effectively reduced by the addition of terminal fairings. Both configurations had a nozzle turning-lip angle of 29.7°, a ratio of annulus gap to base radius of approximately 0.35, and a ratio of annulus gap to base depth of approximately 13.8. These jet-exit configurations were attached to a pylon-mounted model as shown in figure 2. Photographs of the models located in the tunnel test section are presented in figure 3.

For this investigation the model was held at zero angle of attack throughout the Mach number range from 0.80 to 1.28. The average Reynolds number based on

body length was approximately 20×10^6. The jet exhaust was provided by a hydrogen peroxide turbojet-engine simulator (ref. 5). The ratio of primary jet total pressure to free-stream static pressure was varied from 1.00 (jet off) to 8.20.

The instrumentation included a one-component strain-gage thrust balance, a total-pressure probe and a total-temperature probe located in the tailpipe, static-pressure orifices on the concave central base located on a meridian line at angles of 45° and 225°, and an impeller-type electronic flowmeter. The pressures were measured with electrical pressure transducers. The outputs of the pressure transducers, the thrust balance, and the flowmeter were transmitted to and recorded by an automatic digitizer system. The jet stagnation temperature was measured with a pen-trace self-balancing potentiometer. The pressures and forces were converted to coefficient form and ratios by machine computations.

The measured weight flow is estimated to be accurate within ±0.02 pound per second, and the thrust measurements are estimated to be accurate within ±4 pounds of thrust. The estimated accuracy of the pressure measurements is ±2 percent.

RESULTS AND DISCUSSION

Propellant Weight Flow

In figure 4 is presented the variation of weight flow of the hydrogen peroxide propellant with jet total-pressure ratio for configuration I at various Mach numbers. Similar data for configuration II were not obtained owing to instrumentation malfunction.

Base Pressures

The pressure distributions on the concave base are shown in figure 5 and the resulting base thrust coefficients are presented in figure 6. Pressures were measured across the entire base as indicated in figure 1. Since these measurements were symmetrical about the axis of symmetry, only one side is presented.

Reference 1 indicates that the use of a concave base aids in the establishment of a ring-vortex-type flow in the base region, which serves as a more efficient medium for the transmission of pressure from the converging jet flow to the base than would occur in a simple, turbulent wake. For a convergent, annular nozzle such as used in reference 1 the base thrust would be expected to increase uniformly with increasing jet total-pressure ratio. Figure 6 indicates, however, that following an initial increase in base thrust coefficient with increasing jet total-pressure ratio, a rapid decrease occurs at conditions dependent on pressure ratio and Mach number. As pressure ratio is increased beyond this point, the trend reverses and thrust coefficient increases nearly linearly. The fact that the pressure ratio at which this discontinuity occurs decreases with increasing Mach number indicates that the phenomenon is a function of the expansion characteristics of the nozzle.

The decrease in base thrust is believed to be due largely to the fact that the inner lip of the present nozzle inadvertently extended downstream of the throat and thereby formed a slightly divergent shape. An intuitive explanation is that at low values of jet total-pressure ratio (jet slightly supersonic), expansions starting from the outer lip of the nozzle reflect as expansions from the inner lip surface downstream of the minimum, then reflect as compressions from the outer free surface of the jet, and thus increase the convergence of the annular jet which tends to increase base pressure. At the higher values of pressure ratio and with the reduced pressure field on the outer lip associated with the higher values of Mach number, the expansions starting at the outer lip of the nozzle extend beyond the end of the inner lip to the free boundary between the annular jet and the base flow. The expansions are reflected from this free boundary as compressions and cause the streamlines of the annular jet to be less convergent. This reduction in convergence tends to decrease the pressure in the base region.

It is also noted in figure 6 that the rate of increase in thrust coefficient with jet total-pressure ratio appears to be greater at pressure ratios above that at which the discontinuity occurs. An examination of the base pressure distributions (fig. 5) indicates that the character of these curves changes with increasing pressure ratio in a manner consistent with the changes in the slopes of the thrust curves (fig. 6). Inasmuch as at the lower pressure ratios and Mach numbers the distributions are nearly uniform across the concave base, very little or no vortex-type circulation such as described in reference 1 is indicated. At higher pressure ratios and Mach numbers, the presence of a well-defined vortex flow is indicated by the pressure peaks near the center and at the edges of the base. The increased efficiency of pressure transmission to the base by this vortex flow is evidenced by the increased slope of the thrust curve.

It is interesting to note in figures 7 and 8 that no discontinuities occur in the overall thrust-minus-drag coefficient values. This fact indicates that the changes (fig. 6) are due to local phenomena such as described above which do not necessarily influence the overall thrust-minus-drag values. It may also be noted in figure 6 that the terminal fairings favored the formation of the nonuniform pressure pattern since the onset of this pattern occurred at lower pressure ratios and Mach numbers for configuration II than for configuration I.

Nozzle Efficiency

The thrust ratio $\dfrac{C_{(F-D)}}{C_{F,i}}$ may be considered a measure of the overall nozzle efficiency. The variation of thrust ratio with jet total-pressure ratio for configuration I at various Mach numbers is presented in figure 9. Similar information is not presented for configuration II because of incomplete data owing to faulty instrumentation.

Comparison of the thrust ratio for static conditions with the thrust ratios at various Mach numbers indicates the effects of forward speed or external airstream on the nozzle efficiency. It may be seen that for the pressure-ratio range of this investigation, increase in forward speeds reduced the overall

efficiency of the nozzle progressively for a given pressure ratio. The range of pressure ratios used during this investigation did not cover high enough value to obtain maximum efficiencies (except possibly at a Mach number of 0.90). Thus, the best operating pressure ratios for this nozzle are greater than for most conventional nozzles. Although the efficiencies for the supersonic Mach numbers did not reach values greater than about 89 percent during this investigation, the curves indicate that efficiency was increasing continuously with increasing pressure ratio and that values in excess of 90 percent would have been obtained at slightly higher values of pressure ratio.

Effect of Terminal Fairings on Flight Performance

In order to compare the performance of the two configurations under simulated flight conditions, a schedule of engine operating characteristics was assumed as shown in figure 10. These data indicate that the terminal fairings (configuration II) have a slightly detrimental effect on nozzle performance at Mach numbers from 0.80 to approximately 0.95 and a beneficial effect at Mach numbers from 0.95 to 1.28. The thrust-minus-drag coefficient losses at subsonic Mach numbers reached values up to 0.06, whereas the gains at higher speeds reach value as high as 0.13.

The values of $C_{(F-D)}$ for both configurations decreased continuously with increase in Mach number from 0.80 to 1.28, the rates of decrease being greater in the below-sonic range than for the above-sonic range. The thrust-minus-drag coefficient dropped from about 2.6 at a Mach number of 0.80 to about 1.8 at a Mach number of 1.28.

CONCLUSIONS

An investigation at transonic speeds of the performance of a plug nozzle with concave central base, with and without terminal fairings, indicates the following conclusions:

1. The overall efficiency of the configuration without terminal fairings decreased with increase in Mach number in the range of pressure ratios used by conventional turbojet engines.

2. The addition of terminal fairings to the basic nozzle decreased the thrust minus drag at subsonic speeds but increased that for sonic and above-sonic speeds within the range of Mach numbers covered in this investigation.

3. The flow pattern at the concave central base was influenced by Mach number, jet total-pressure ratio, and the terminal fairings. The base flow pattern affected the concave-base thrust but not the overall thrust minus drag.

Langley Research Center,
National Aeronautics and Space Administration,
Langley Station, Hampton, Va., March 21, 1963.

REFERENCES

1. Corson, Blake W., Jr., and Mercer, Charles E.: Static Thrust of an Annular Nozzle With a Concave Central Base. NASA TN D-418, 1960.

2. Mercer, Charles E., and Simonson, Albert J.: Effect of Geometric Parameters on the Static Performance of an Annular Nozzle With a Concave Central Base. NASA TN D-1006, 1962.

3. Swihart, John M., Norton, Harry T., Jr., and Schmeer, James W.: Effect of Several Afterbody Modifications Including Terminal Fairings on the Drag of a Single-Engine Fighter Model With Hot-Jet Exhaust. NASA MEMO 10-29-58L, 1958.

4. Willis, Conrad M., and Norton, Harry T., Jr.: Effect of Afterbody Terminal Fairings on the Performance of Plug-Type Exhaust Nozzles at Transonic Speeds. NASA TM X-762, 1963.

5. Runckel, Jack F., and Swihart, John M.: A Hydrogen Peroxide Hot-Jet Simulator for Wind-Tunnel Tests of Turbojet-Exit Models. NASA MEMO 1-10-59L, 1959.
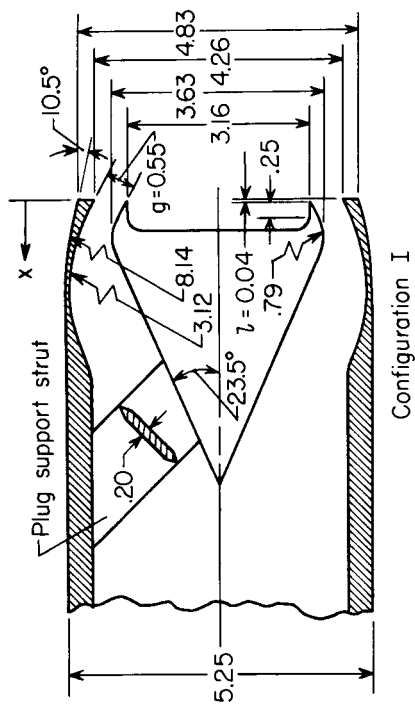
Fairing Coordinates

x	z	R2
-2.59	0.48	2.59
-2.38	.58	2.53
-1.33	1.05	2.26
-.80	1.20	2.15
-.49	1.26	2.13
-.28	1.27	2.13
0	1.25	2.13
.42	1.10	―――
1.47	.64	―――

Plug Coordinates

x	R1
0.04	1.58
.16	1.64
.28	1.70
.43	1.77
.69	1.82
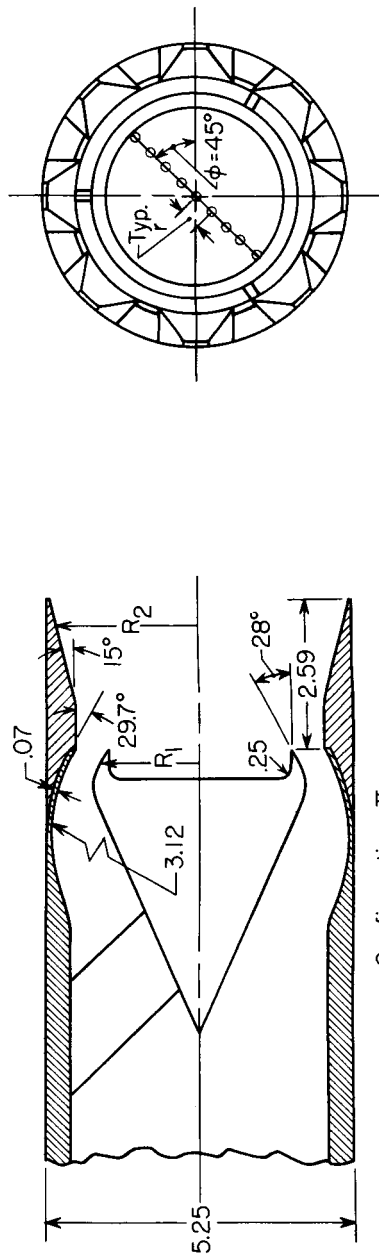
Orifice Locations

Row	r	r/R
$\phi = 45°$ and 225°	0.00	0.00
	.38	.24
	.75	.48
	1.13	.72
	1.50	.95

Configuration I

Plug support strut

g = 0.55
3.12
8.14
23.5°
l = 0.04
.79
.25
.20
10.5°
4.83
4.26
3.63
3.16

Configuration II

R2
R1
15°
29.7°
28°
2.59
.25
.07
3.12

5.25

Figure 1.- Geometry of models. All dimensions in inches unless otherwise noted.
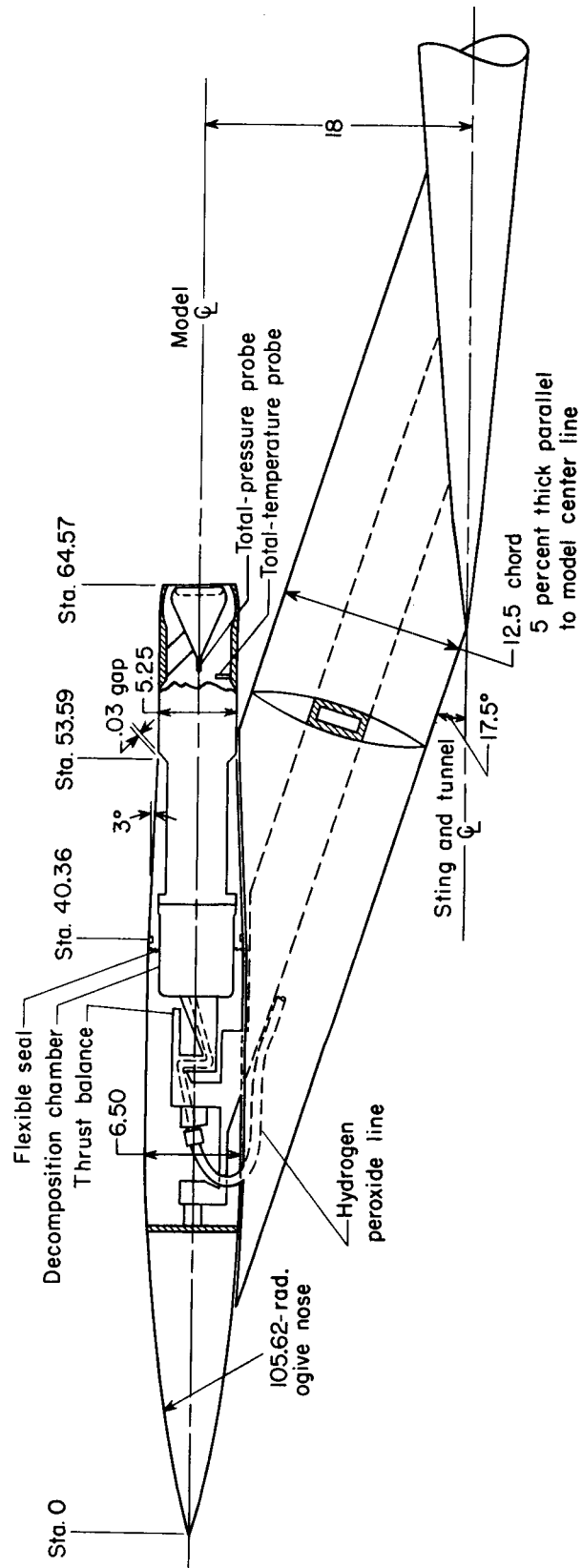
Figure 2.- Model installation - basic afterbody. All linear dimensions in inches.
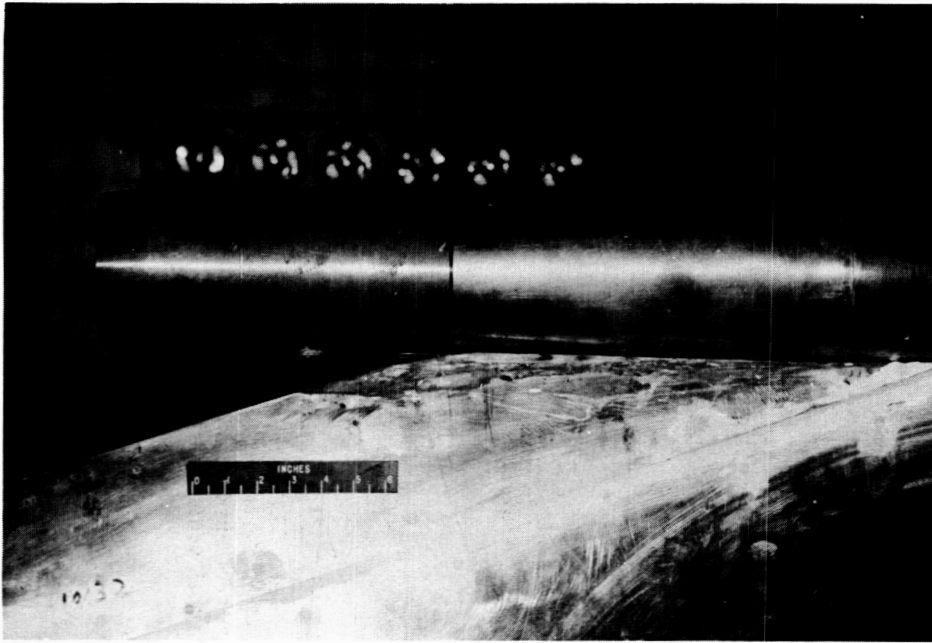
Side view

L-61-5976

Three-quarter rear view

L-61-5978

(a) Configuration I.

Figure 3.- Photographs of models.
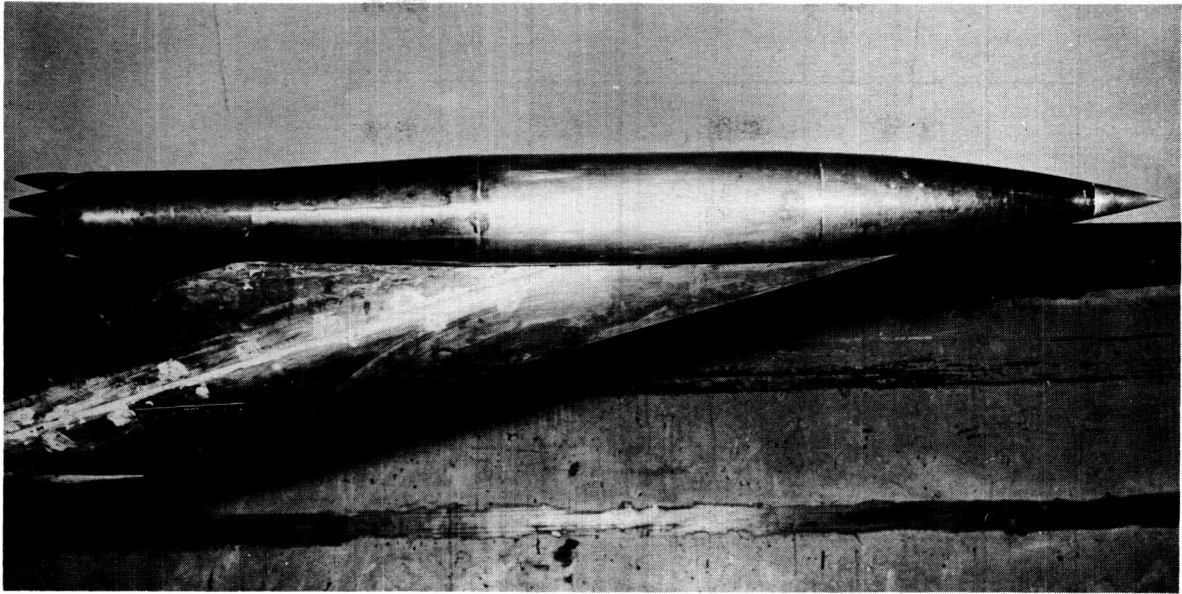
Side view

L-61-5977
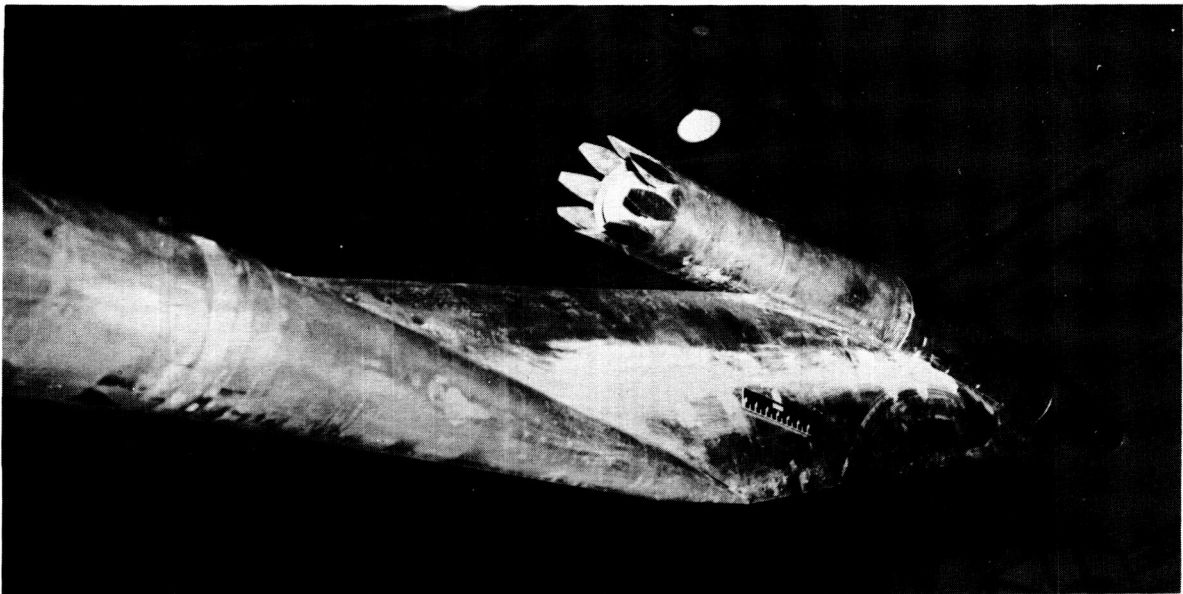
Three-quarter rear view

L-61-5979

(b) Configuration II.

Figure 3.- Concluded.
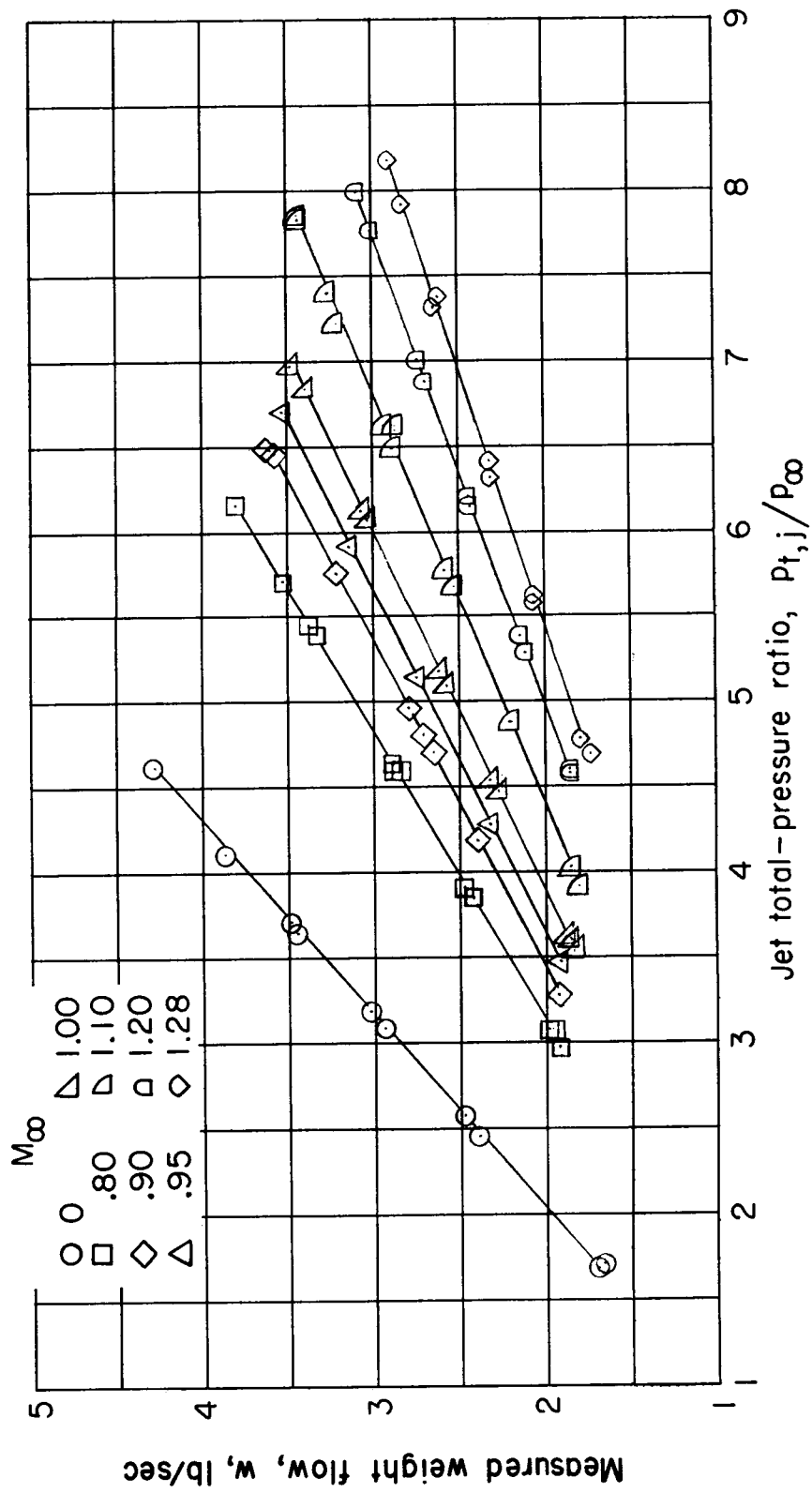
Figure 4.- Variation of measured propellant weight flow with jet total-pressure ratio. Configuration I.
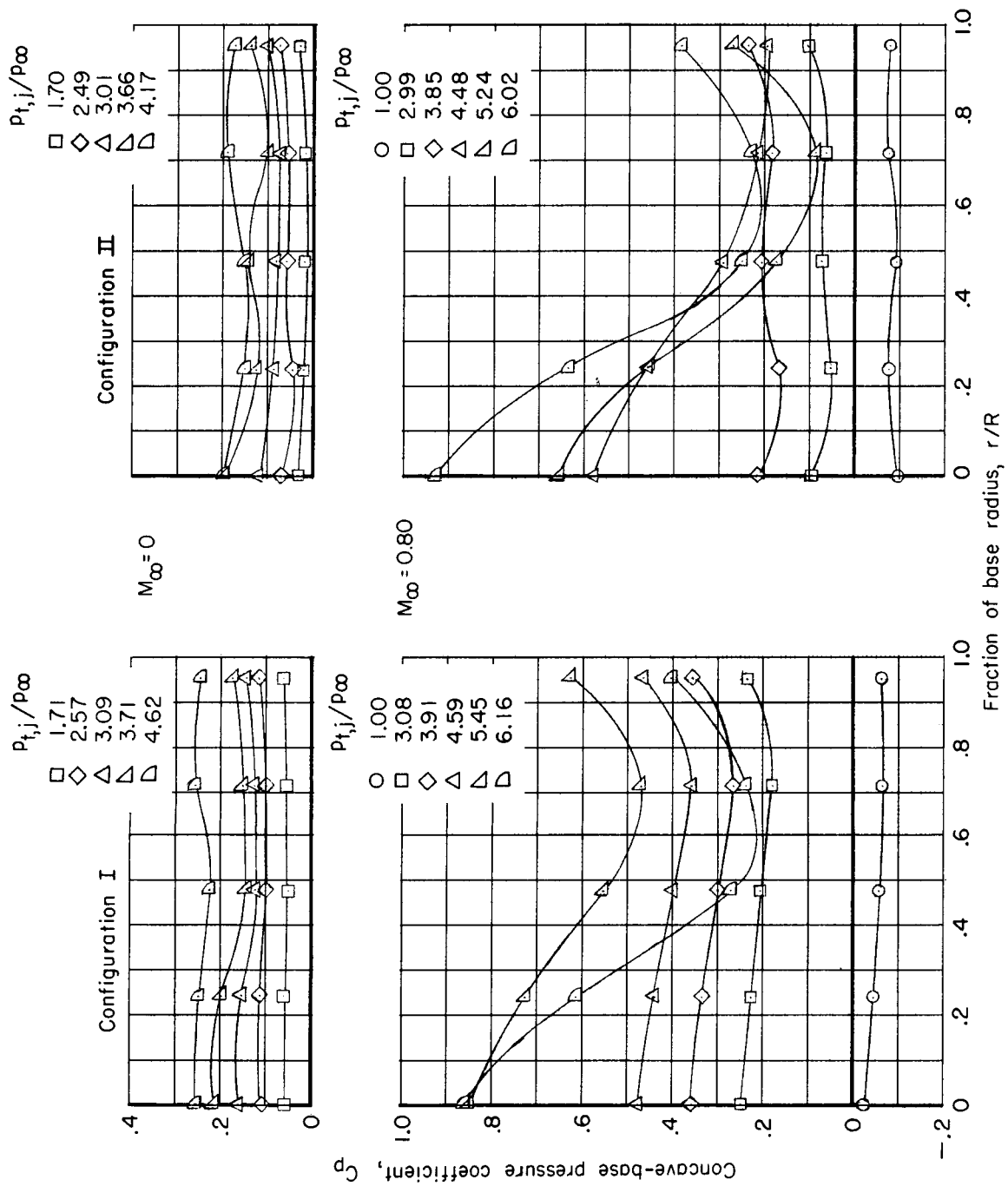
Figure 5.- Pressure distributions on concave central base for various jet total-pressure ratios and Mach numbers.

(a) $M_\infty = 0$ and 0.80.

13
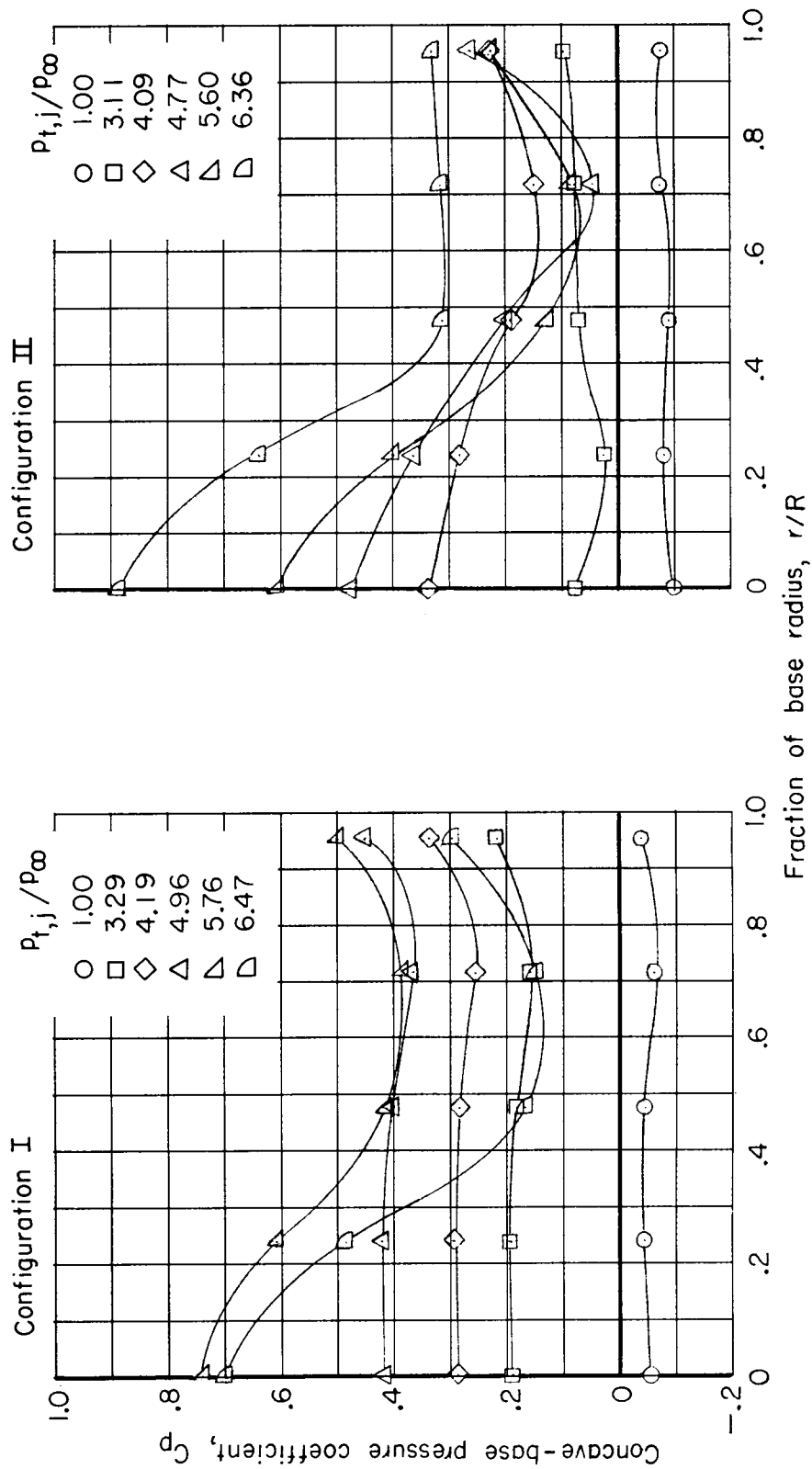
(b) $M_\infty = 0.90$.

Figure 5.- Continued.
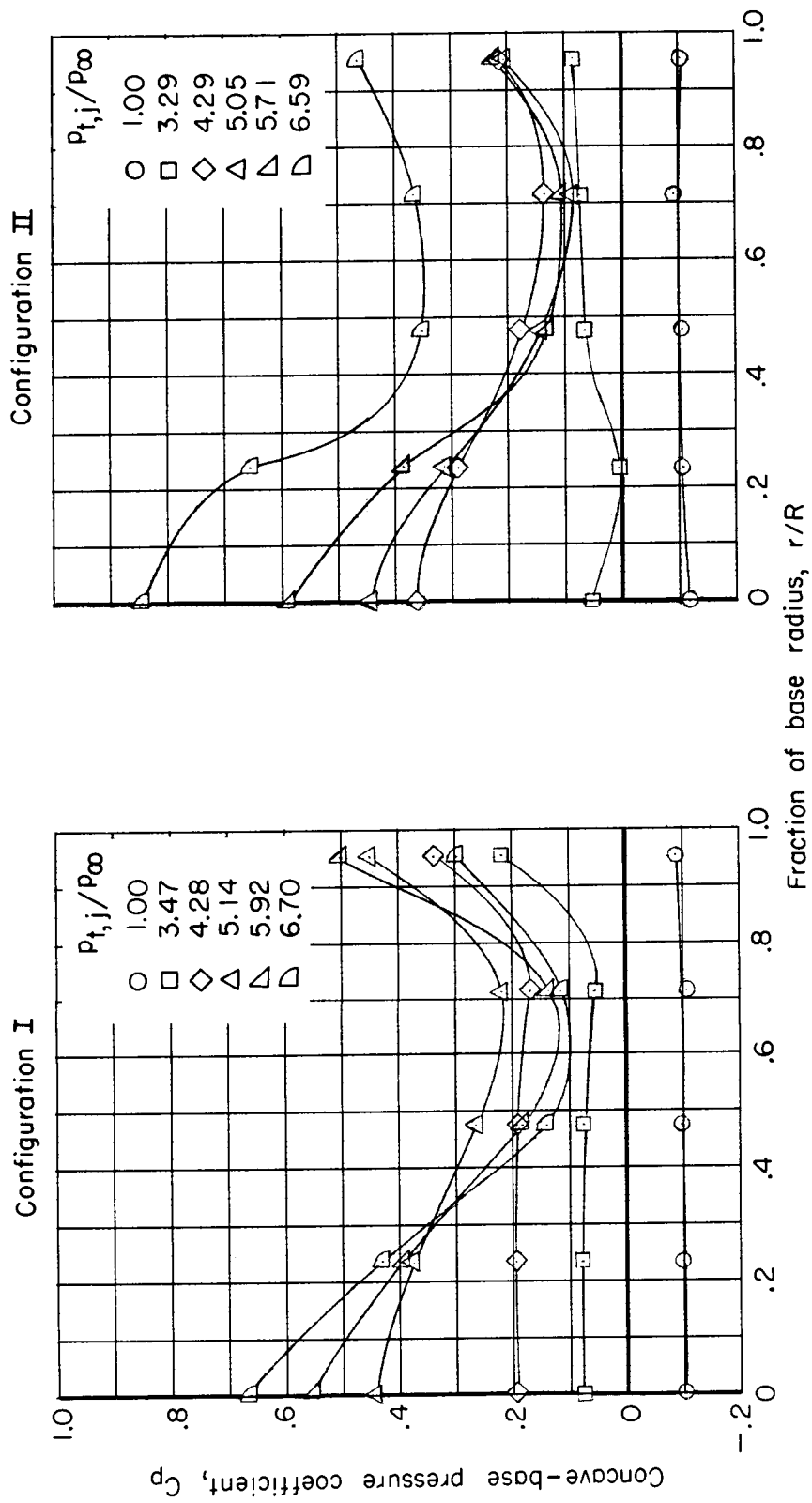
(c) $M_\infty = 0.95$.

Figure 5.- Continued.
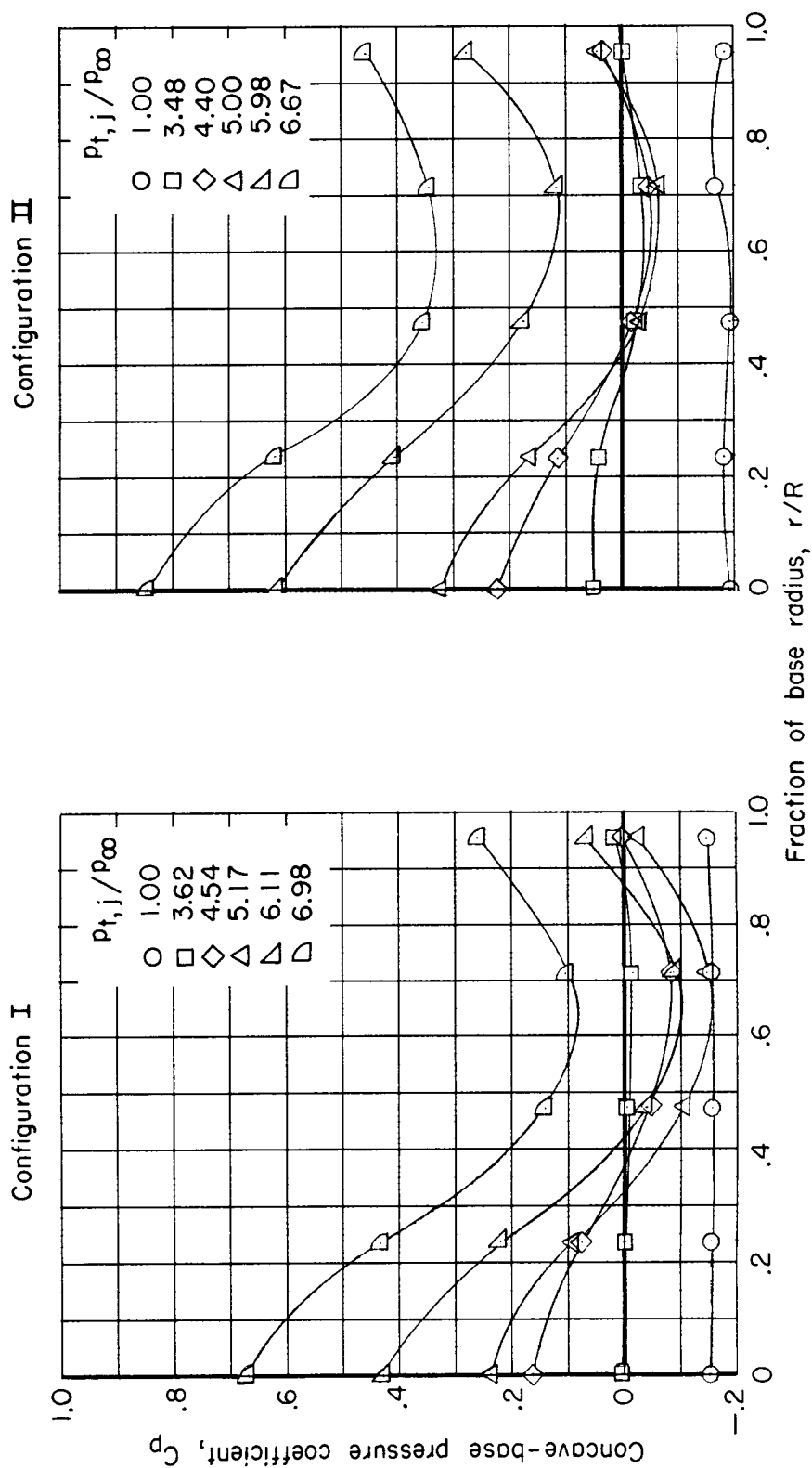
(d) $M_\infty = 1.00$.

Figure 5.- Continued.

16
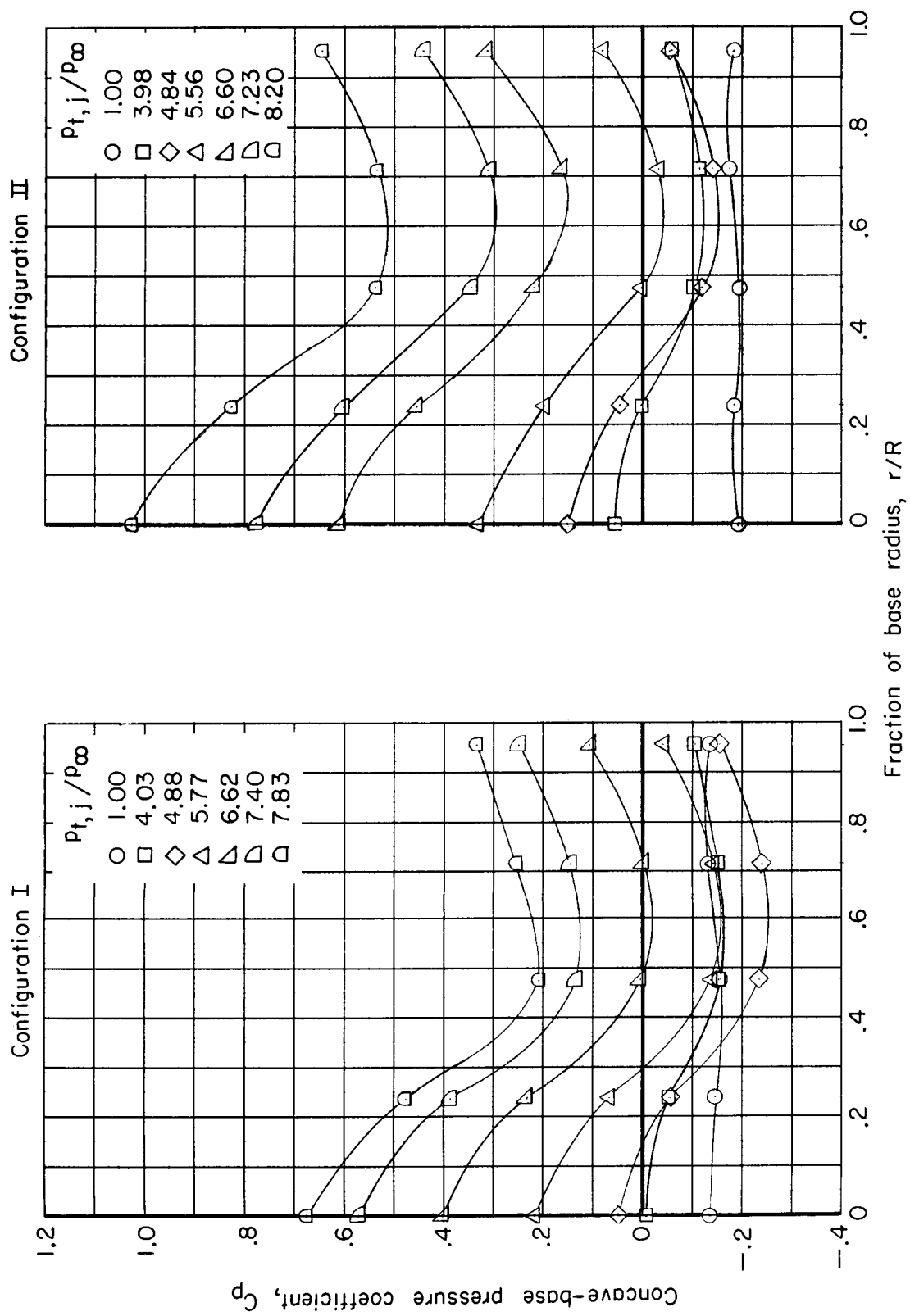
(e) $M_\infty = 1.10$.

Figure 5.- Continued.

17
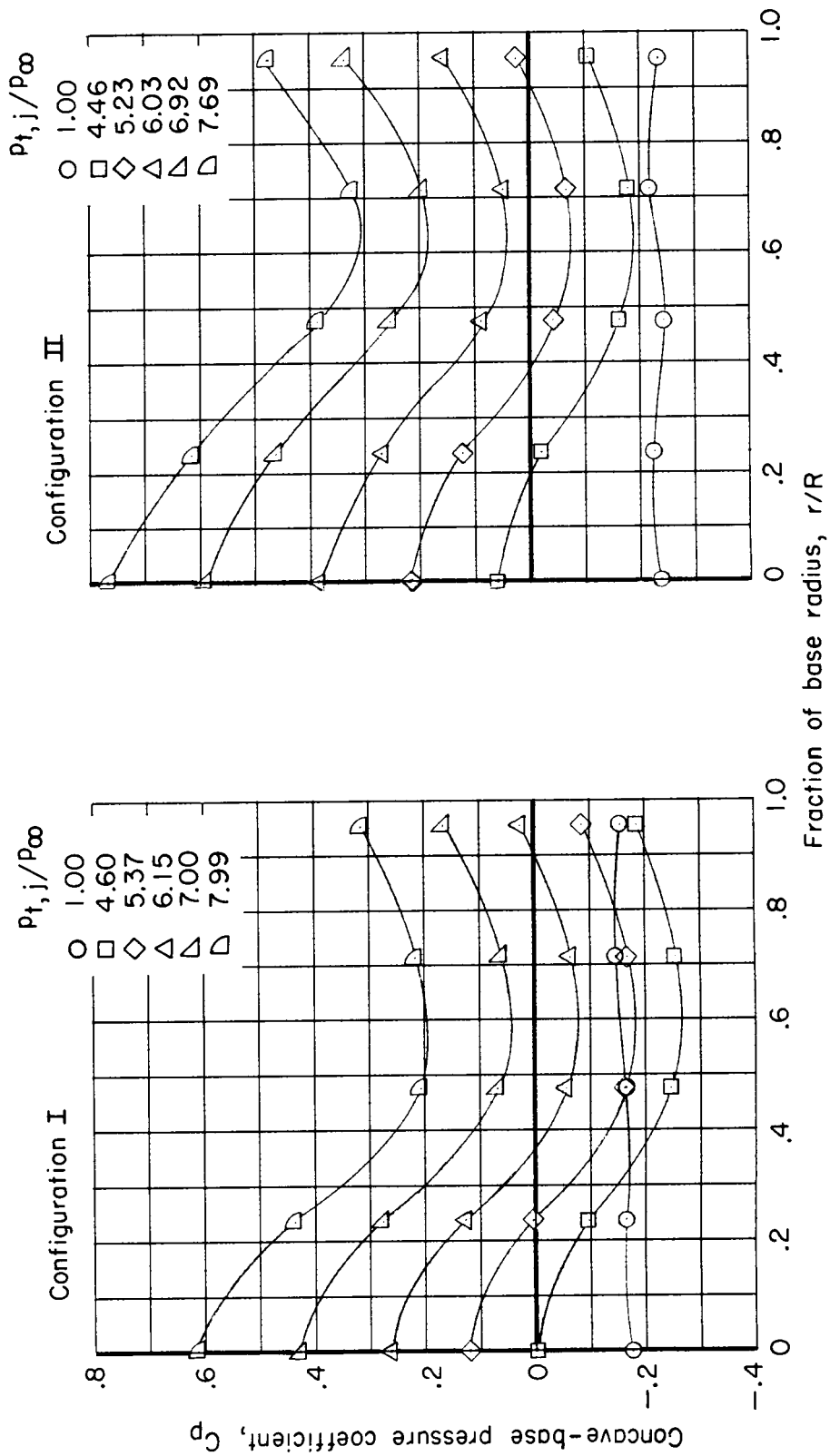
(f) $M_\infty = 1.20$.

Figure 5.- Continued.
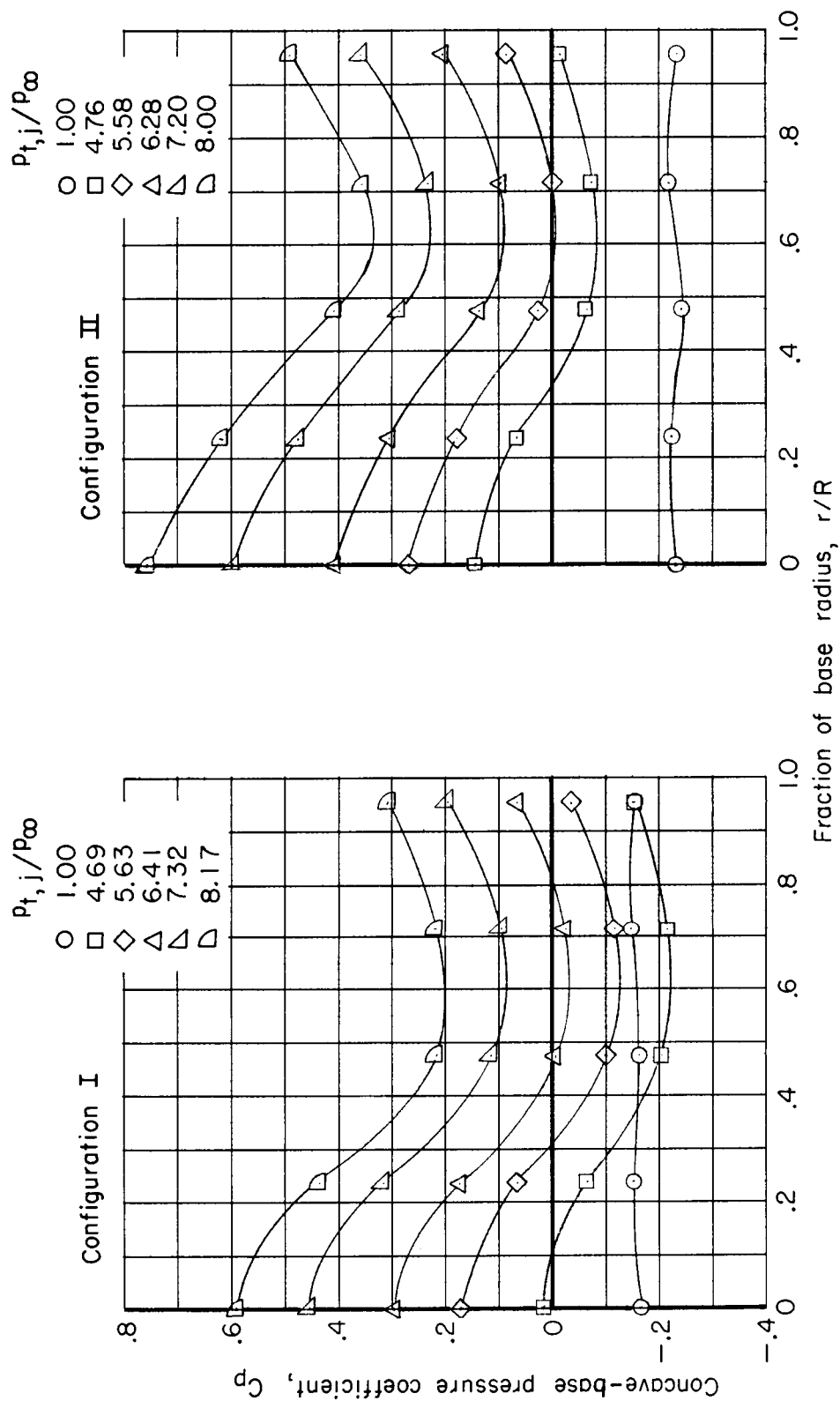
(g) $M_\infty = 1.28$.

Figure 5.- Concluded.
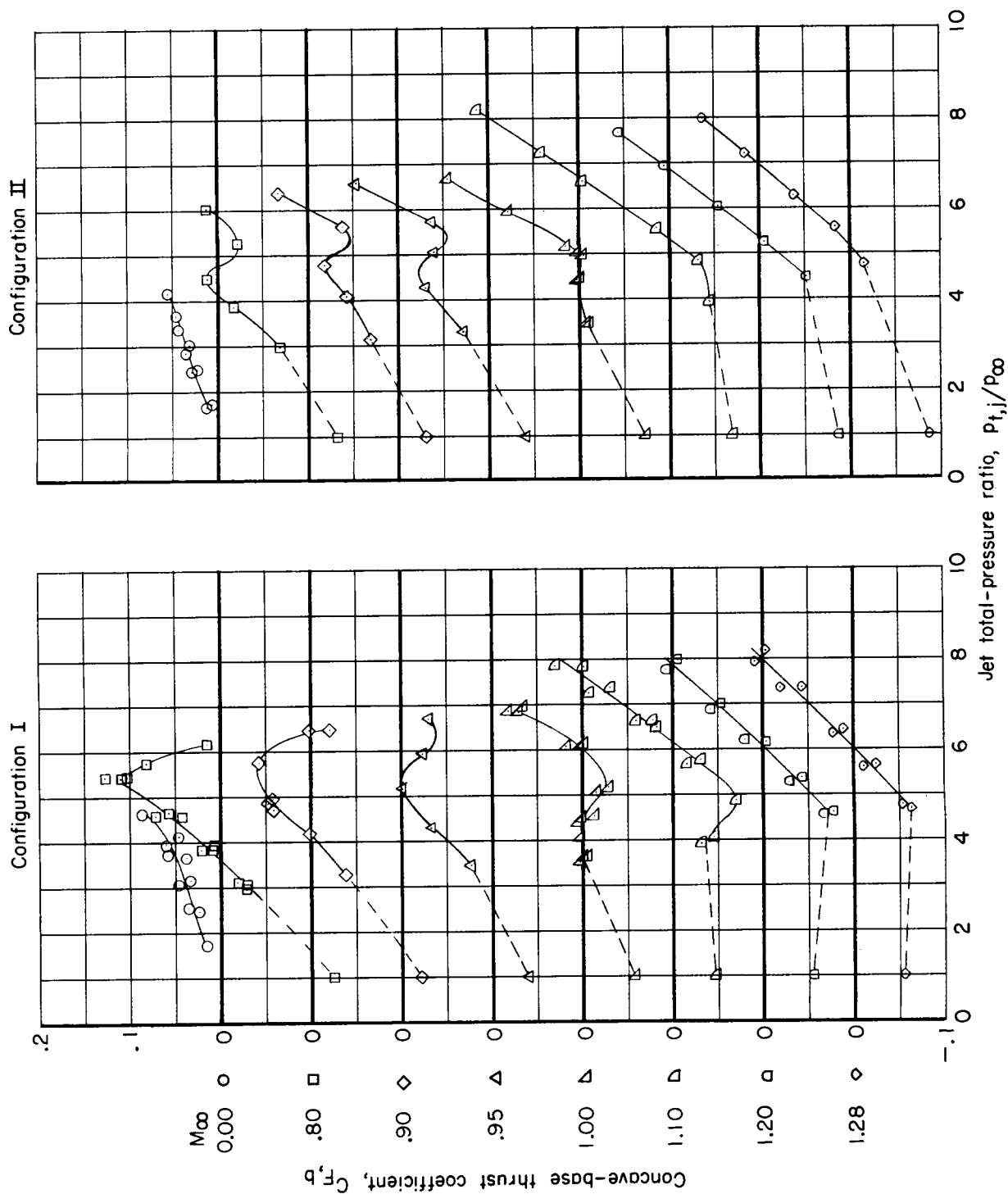
Figure 6.- Variation of concave-base thrust coefficient with jet total-pressure ratio for various Mach numbers.
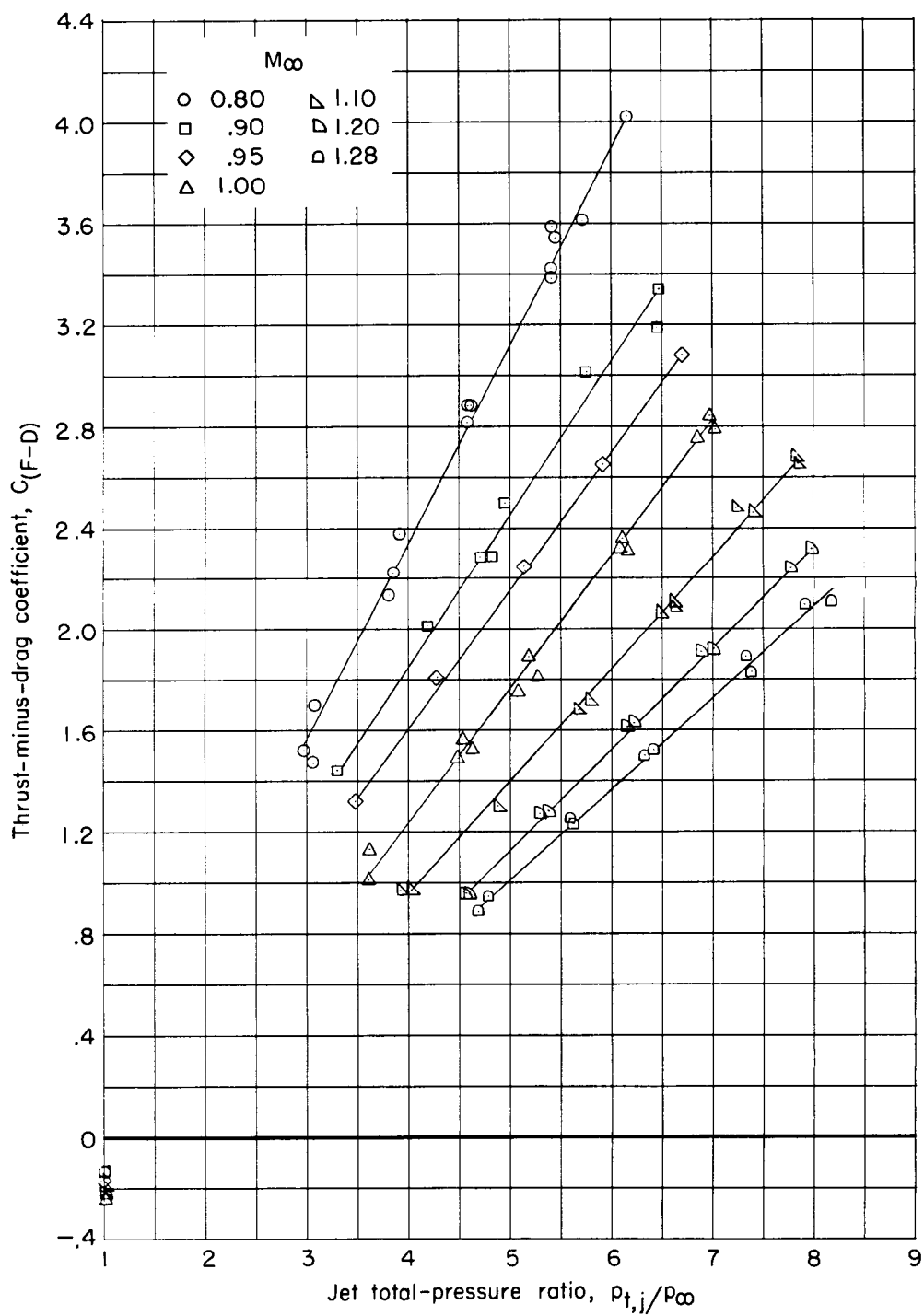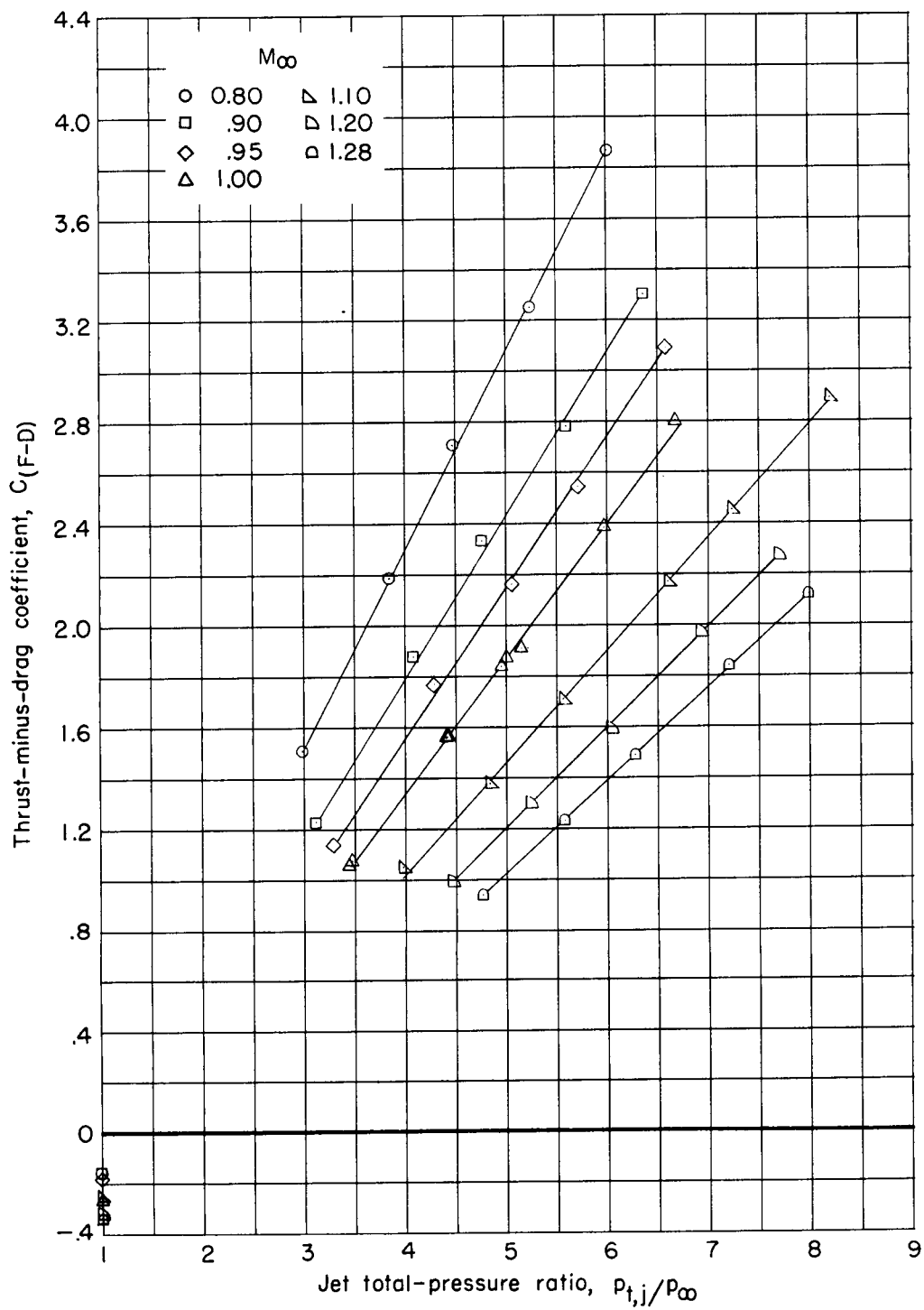
20
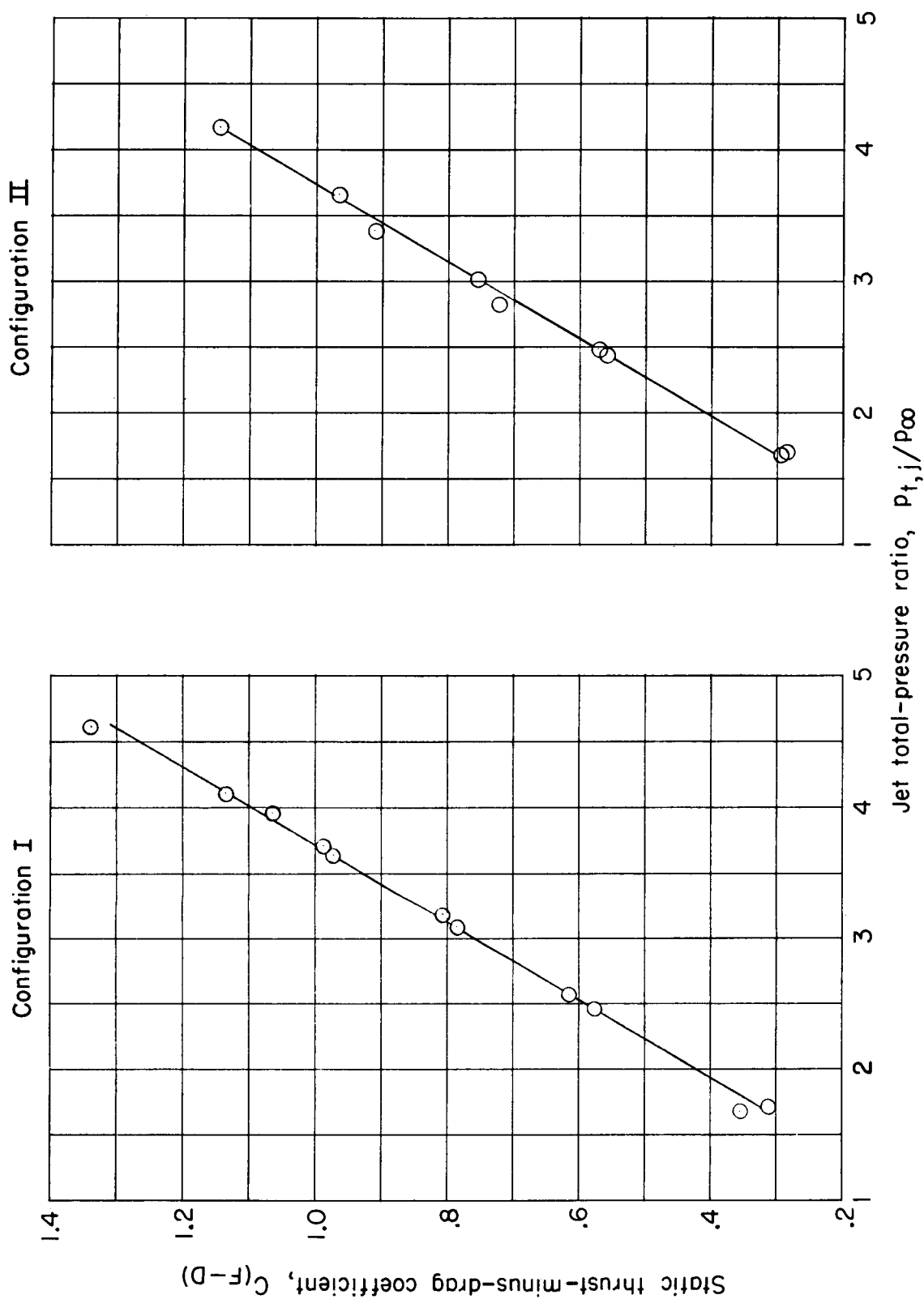
Figure 7.- Variation of thrust-minus-drag coefficient with jet total-pressure ratio in quiescent air.

(a) Configuration I.

Figure 8.- Variation of thrust-minus-drag coefficient with jet total-pressure ratio for various Mach numbers.
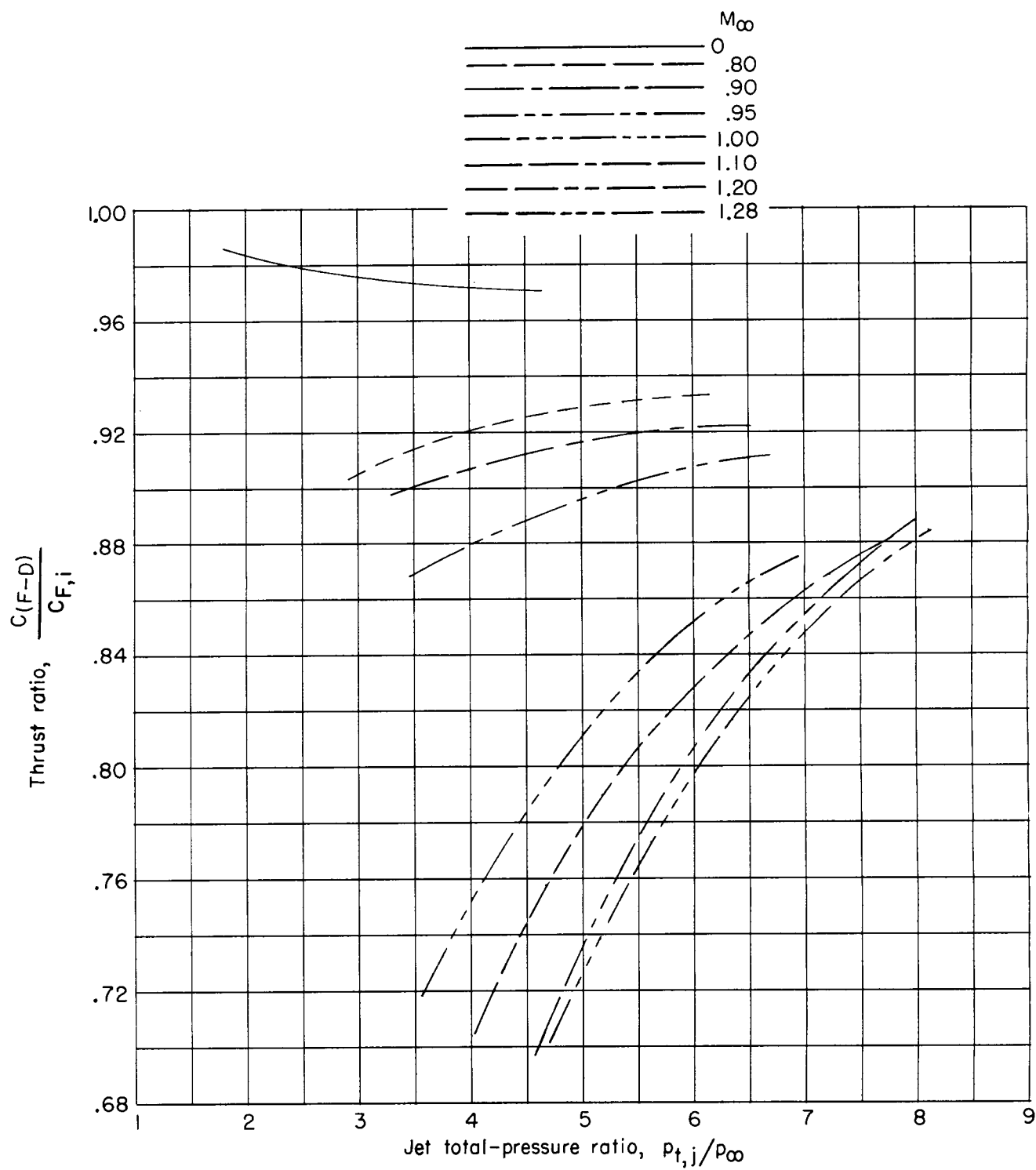
(b) Configuration II.

Figure 8.- Concluded.

Figure 9.- Variation of thrust ratio with jet total-pressure ratio for various Mach numbers. Configuration I.
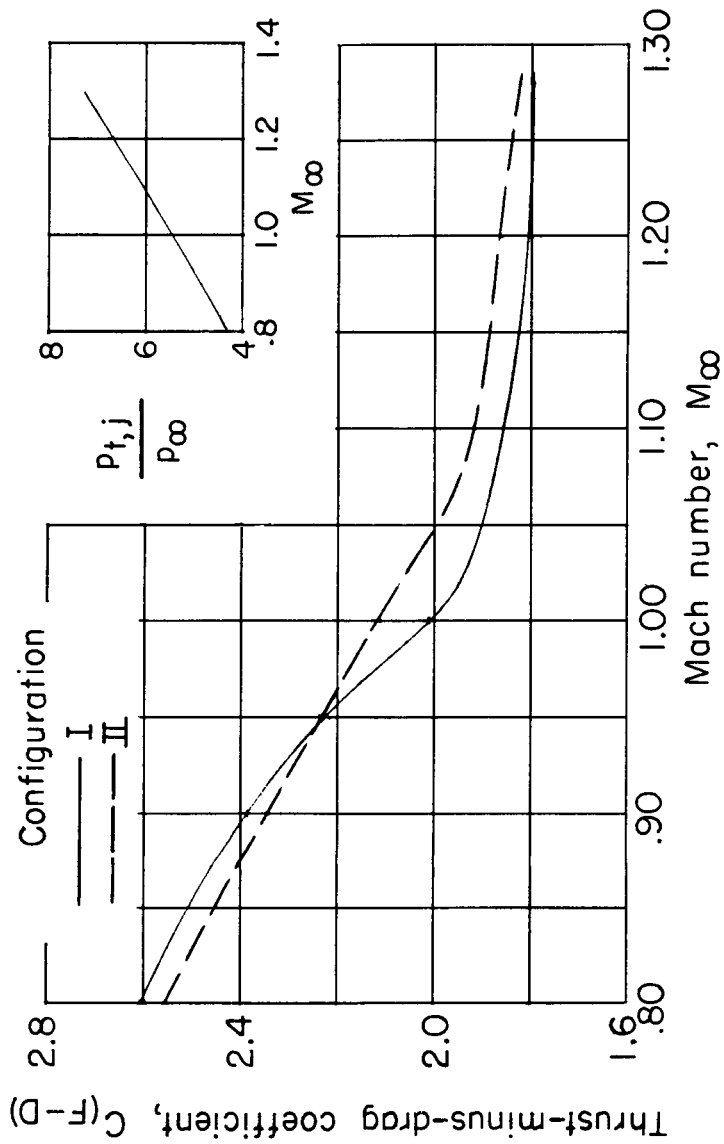
Figure 10.- Effect of Mach number on thrust-minus-drag coefficient. Data are presented for jet total-pressure ratios corresponding to the schedule with Mach number for a typical turbojet-engine configuration.